PCCP

Accepted Manuscript

ROYAL SOCIETY OF CHEMISTRY

www.rsc.org/pccp

Alternative mechanisms for O_2 release and O-O bond formation in the oxygen evolving complex of photosystem II.

Xichen Li [a,b] and Per E. M. Siegbahn[b,*]

[a]College of Chemistry, Beijing Normal University, 100875, Beijing, China [b] Department of Organic Chemistry, Arrhenius Laboratory, Stockholm University, SE-106 91, Stockholm, Sweden.

*Corresponding author: Per Siegbahn, e-mail: ps@organ.su.se, telephone: +46-8-16 26 16.

Abstract

In a previous detailed study of all the steps of water oxidation in photosystem II, it was surprisingly found that O_2 release is as critical for the rate as O-O bond formation. A new mechanism for O_2 release has now been found, which can be described as an opening followed by a closing of the interior of the oxygen evolving complex. A transition state for peroxide rotation forming a superoxide radical, missed in the previous study, and a structural change around the outside manganese are two key steps in the new mechanism. However, O_2 release may still remain rate-limiting. Additionally, for the step forming the O-O bond, an alternative, experimentally suggested, mechanism was investigated. The new model calculations can rule out the precise use of that mechanism. However, a variant with a rotation of the ligands around the outer manganese by about 30^o will give a low barrier, competitive with the old DFT mechanism. Both these mechanisms use an oxyl-oxo mechanism for O-O bond formation involving the same two manganese atoms and the central oxo group (O5).

I. Introduction

Water oxidation in nature is catalyzed by the oxygen evolving complex (OEC) in photosystem II (PSII), containing four manganese and one calcium connected by oxo bridges. For the understanding of this process computational modeling studies have played a major role. A theoretically determined structure of the OEC was suggested in 2008 [1], where information from earlier low-resolution X-ray structures [2, 3] was used. This structure was essentially confirmed by a high-resolution structure in 2011 [4], where the only difference was the positioning of Asp170. Very recently the same group obtained a structure of the S_1

state using a free-electron laser [5], showing even better agreement with the corresponding DFT structure. An oxo-oxyl mechanism for O-O bond formation was suggested based on DFT calculations in 2006 [6], which was slightly refined in 2009 [7]. Recent water exchange experiments using a W-band ^{17}O-ELDOR detected NMR spectroscopy [8] for the substrate oxygen positions in the S_2 state have confirmed the most important parts of that mechanism. The quantum chemical structures have been confirmed by experiments for both the S_2 and the S_3 states. A comparison of the structures of the S_2 state suggested by DFT modeling [9, 10] and by spectroscopic experiments [11] is shown in Fig.1, and for the corresponding S_3 structures [10, 12, 13] in Fig.2. The only visible difference is a slight rotation of the His residue, but this has negligible energetic consequences and was therefore outside the goal of the DFT modeling.

Over the years, a variety of different mechanisms for O-O bond formation have been suggested. Most noteworthy of these is the attack of a water molecule, either free of bound to calcium, on an Mn(V)=oxo or Mn(IV)-oxyl state, see for example [14, 15]. This mechanism was compared to the one above and was ruled out by model model calculations in 2006 [6], since the computed barrier was more than 10 kcal/mol higher, which is much more than the uncertainty of the methods. More recently, spectroscopic experiments have given very strong arguments against the nucleophilic water attack mechanism [16]. New information favoring this mechanism appears to be absent in the literature since a couple of years. The only alternative scenario still advocated in the literature is the use of the low-oxidation paradigm [17]. This type of mechanism has been found very unfavorable in all investigations of the present type. Recently, a thorough investigation of the oxidation states of the OEC using a large number of spectroscopic techniques was presented [18]. The analysis strongly argues against the low-oxidation paradigm.

The most complete mechanism for all the steps in water oxidation in PSII, including oxidations, proton release pathways, O-O bond formation and O_2 release was published a year ago [10]. A surprising feature of this mechanism was that the final step, involving O_2 release and water binding, had the highest barrier. This complicated step is composed of several parts. After O-O bond formation leading to a bridging peroxide, O_2 is first released in an endergonic step. This is followed by a proton transfer from a water bound to calcium, over an intermediate water, to a hydroxide bound to the outer manganese. In the next two substeps, the hydroxide on calcium moves into the cavity between the manganese centers, and a new water molecule becomes bound to calcium [10]. The highest barrier was

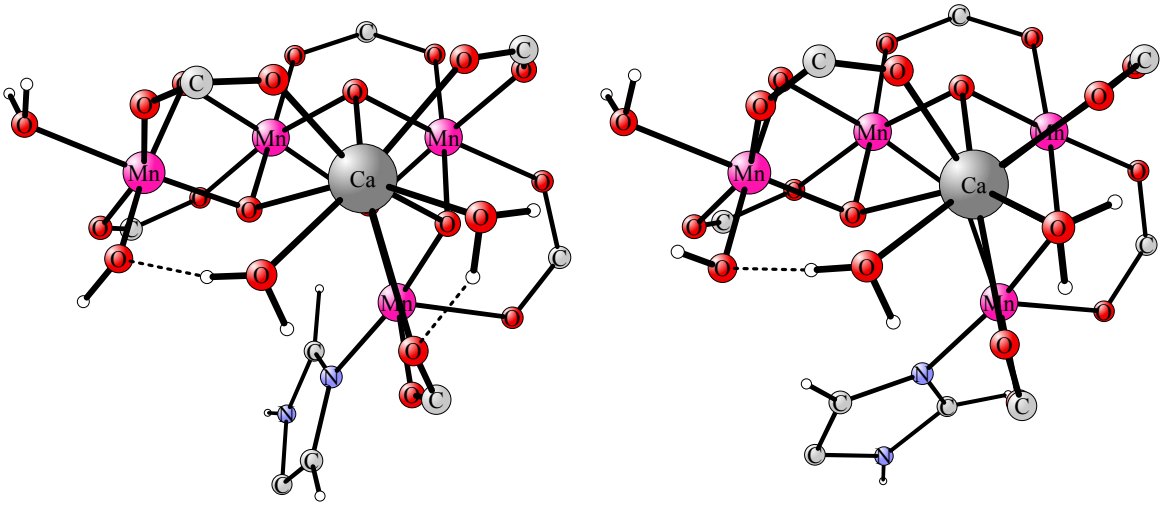

Figure 1: The previously DFT(B3LYP)-optimized structure for the S_2-state [9, 10] is shown to the left and the structure suggested after a spectroscopic analysis is shown to the right [11]

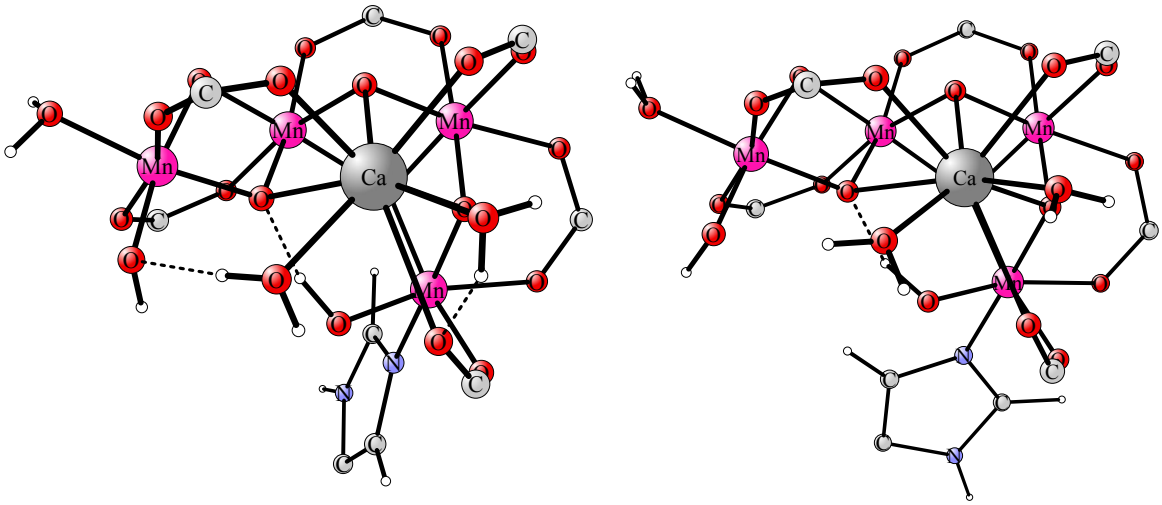

Figure 2: The previously DFT(B3LYP)-optimized structure for the S_3-state [12, 10] is shown to the left and the structure suggested after a spectroscopic analysis is shown to the right [13]

found for the proton transfer from the calcium bound water, with a value of 14.0 kcal/mol counted from the resting S_3 state. This barrier actually made this step rate-limiting for the entire water oxidation mechanism, since the barrier for O-O bond formation was only 11.3 kcal/mol. A large effort was spent investigating whether a concerted O_2 release with water binding would be advantageous, but this was not successful.

The finding that the proton transfer step after O_2 release should be rate-limiting remained quite surprising, and during the past year new investigations were made trying to

find a better mechanism for this step. In the present communication, a new mechanism for all steps of O_2 release is presented.

It should finally be emphasized that a full comparison to other theoretical work is not within the scope of the present paper. The starting point for the present study is one of the previously suggested mechanisms, the one described above. For other theoretical work on water oxidation in PSII the reader is referred to recent reviews [10, 17, 19], where different suggestions have been discussed in detail.

II. Methods and models

The Density Functional Theory (DFT) calculations discussed here were performed in essentially the same way as described in detail previously [10]. The hybrid functional B3LYP* [20, 21] was used with polarized basis sets for the geometries (lacvp*), large basis sets for energies (cc-pvtz(-f)/lacv3p+), and a surrounding dielectric medium with dielectric constant equal to 6.0 (basis lacvp*). The performance of the B3LYP functional for the present type of problems has been reviewed [22, 23, 24], indicating a typical accuracy within 3-5 kcal/mol, normally overestimating barriers. Dispersion effects were added using the empirical D2 formula of Grimme [25]. A difference to the previous study is that full geometry optimizations (except for fixed backbone atoms) of the transition states were made at the same level as for the other structures, which involved calculating Hessians for the full model, not truncated ones as before. Hessians were also done for all intermediate structures, from which zero-point effects were obtained. An Internal Reaction Coordinate (IRC) was not computed since this is not trivial for the present large model with high spin and fixed coordinates. Instead the reaction was followed from the TS to the products in small steps by sequential reoptimizations. This has been done both for the proton transfer step and for the O2-release step. The expected products described in the text were obtained in both cases. A spin-correction of -3.5 kcal/mol was added for the S_4-state structures. This correction was obtained from using a Heisenberg spin-Hamiltonian formalism [26, 27] for the S_4^{-1} oxygen radical state. For the release of dioxygen an entropy effect of -12 kcal/mol was added taken from the gain of translational entropy, just like in our previous papers. When spin is reffered to, it means spin-density from a Mulliken popualtion analysis. The calculations were performed with the Jaguar and Gaussian programs [28, 29].

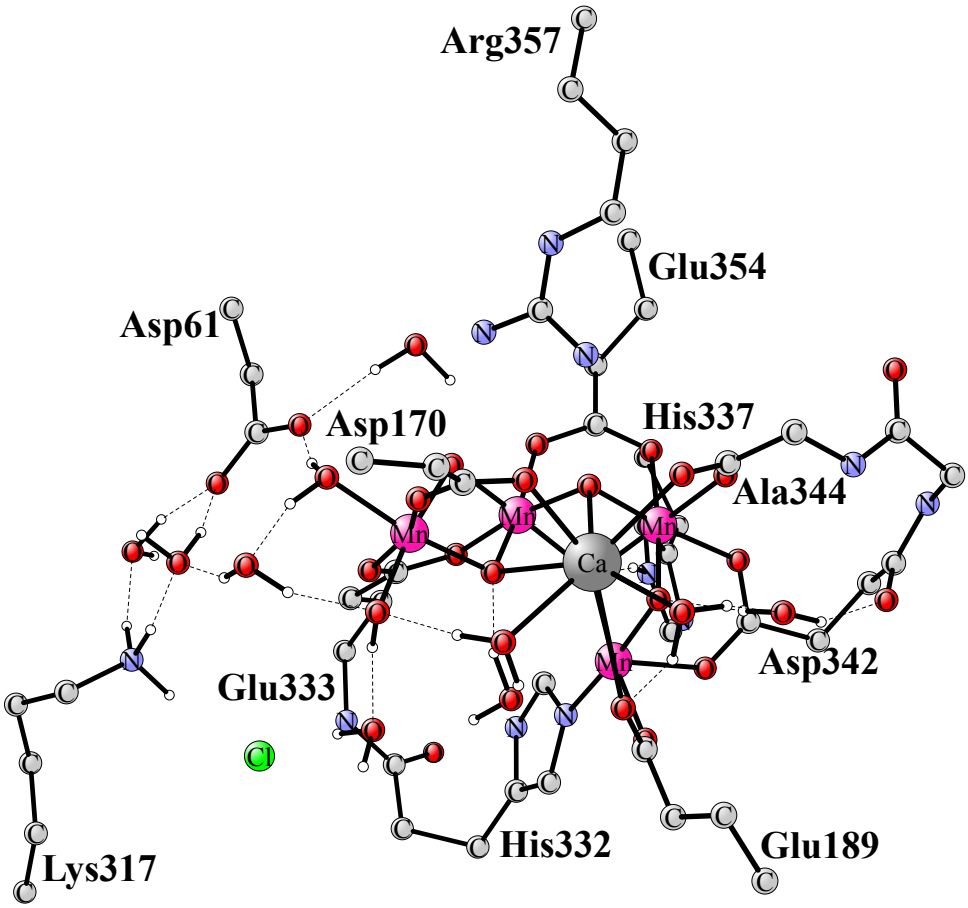

Figure 3: The full model used in the present study, mainly illustrating the amino acids included. Most hydrogen atoms are left out.

The quantum chemical cluster model chosen for the present applications is the same as the one used in the most recent studies [10]. The model is based on the high-resolution (1.9 Å) structure by Umena et al [4], and is seen for the S_2-state in Fig.3, where only the most important atoms are shown. The coordinates for the fully optimized (except the fixed backbone atoms) 200 atom structures are given as supplementary material. The amino acids included in the model are first the directly binding amino acids, Asp170, Glu189, His332, Glu333, Asp342, Alal344 and Glu354. The second shell residues Asp61, His337 and Arg357 and the region around the chloride are also included. This region contains, besides chloride, also Lys317 and three water molecules, forming a hydrogen bonding network, as in the X-ray structure.

III. Results.

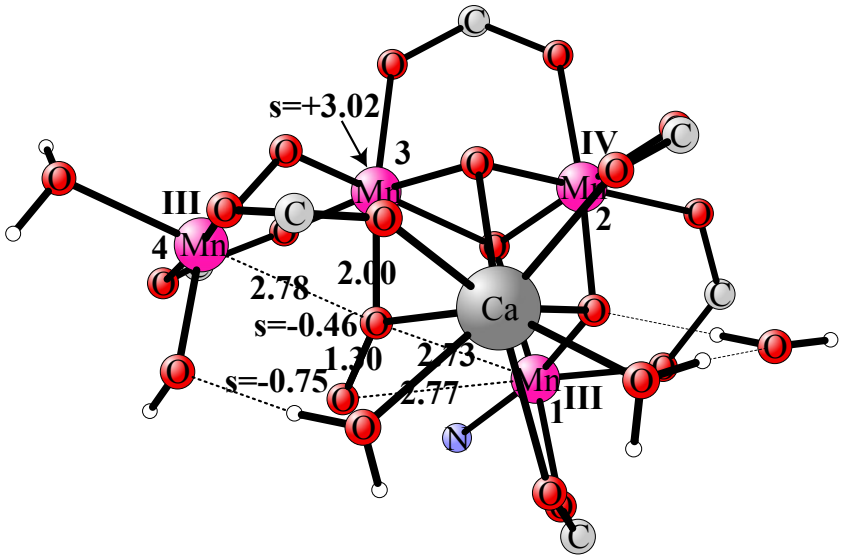

Figure 4: The new rate-limiting transition state for O_2 release. Only the most important atoms are shown.

a. O_2 release.

The present re-investigation of the O_2 release step started out with an improved calculation of the barrier for the O-O bond formation step. In the previous study, the geometry optimization was done by a scan of the O-O coordinate and zero-point effects were taken from smaller models, since calculations of the full Hessians were considered too time-consuming for the large 200 atom model. In the present study a full geometry optimization was actually made for the large model, and an improved spin-correction from -2.8 to -3.5 kcal/mol was also obtained. This improved description decreased the barrier from 11.3 to 9.1 kcal/mol. The thermodynamics for peroxide formation changed from +0.8 to -1.0 kcal/mol.

Already in the first step of the actual O_2 release pathway, the new mechanism deviates strongly from the previous one. In the previous study, O_2 was released endergonically by 6.3 kcal/mol in a barrierless pathway (the TS was missed) with gradually increasing entropy gain. In the new pathway a TS was found between the starting peroxide and the superoxide radical. The barrier is 11.0 kcal/mol, including an entropy effect of -2.0 kcal/mol, obtained from the calculated Hessians. The TS structure is shown in Fig.4. The distance between Mn1 and the outer oxygen of O_2 has now increased from 1.86 Å to 2.77 Å, and the distance between Mn1 and the inner oxygen (bound also to Mn3) has changed from 2.71 Å to 2.73 Å. The spins on the oxygens have increased from essentially zero to -0.75

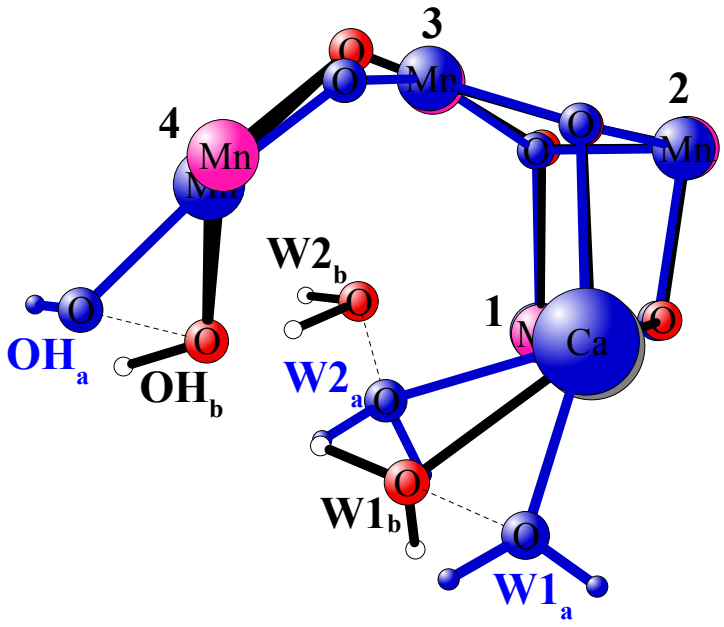

Figure 5: A comparison of the previous (in blue) and present (in red) interior of the OEC just after O_2 has been released. The subscripts a and b are used for the old and new positions, respectively. Only the most important atoms are shown.

and -0.46, indicating a fully formed superoxide radical. The spin on Mn1 has increased from 3.14 (Mn(IV)) to 3.92 (Mn(III)). At the TS structure there is not yet any significant gain of entropy. Already directly after the TS, an outside water moves into the cavity to replace O_2. The O_2 release leads to a gradual increase of the entropy and thereby a decrease of the free energy until O_2 has entirely left the cluster, when the energy is 6.5 kcal/mol higher than for the peroxide reactant. The structure for this point is shown in Fig.5, where it is compared to the corresponding structure from the previous study. As seen in the figure, there are rather large differences between the structures. The entering water molecule (**W2**) is now much deeper into the cavity, with distances of 2.40 Å, 2.46 Å and 3.13 Å to Mn1, Mn3 and Mn4, respectively. The spin has now increased on O_2 to -2.00, and on Mn3 it has increased from 2.88 (Mn(IV)) for the peroxide to 3.89 (Mn(III)). An important feature of the new mechanism is thus that a water enters much earlier into the cavity than previously, where it did not become bound until after the proton transfer from the calcium bound water. Another important difference, seen in Fig.5, is that there is a structural change around Mn4. In the new structure, the ligands form a trigonal bipyramidal structure around Mn4 in contrast to the square pyramidal structure found for the reactant before O_2 release, In the previous study, the Mn4 structure remained square

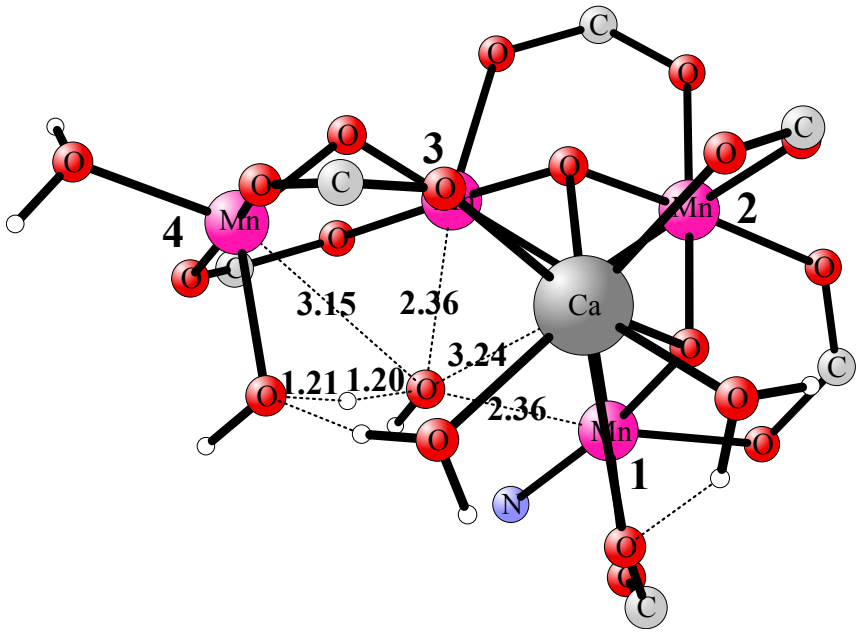

Figure 6: Transition state for proton transfer after O_2 release. Only the most important atoms are shown.

pyramidal throughout this step. As a result of the structural change in the new mechanism, there is a quite significant difference in the position of the hydroxide on Mn4. The distance between the oxygens of the hydroxide and the water in the center of the cavity goes from 4.2 Å in the old structure to 2.5 Å, which is in hydrogen bonding distance.

In the previous study, the next step of proton transfer from a water on calcium to the hydroxide on Mn4 had a very high barrier of 14.0 kcal/mol. With the above structural change around Mn4, it is now possible to move the proton from the water to the hydroxide essentially without a barrier, see Fig.6. At the optimized enthalpic transition state point there is a small barrier, using the smaller basis set. However, when the basis set is increased, and dielectric and zero-point effects are added, the barrier disappears. Still, this point is given in the diagram with an energy of 4.0 kcal/mol. In the next step, the same product as in the previous study is then formed in an exergonic step. Before the resting S_0 state is formed a proton on a water on Mn4 leaves to the lumen, in a process which was assumed to use the same mechanism as in the previous study and is therefore not discussed here.

The energetics from S_3 to S_0 is shown in Fig.7, both for the new (in red) and the old mechanism (in black). It can be seen that the rate-limiting barrier for this transition has now moved from the proton transfer to the O_2 release step. The barrier has gone down from 14.0 to 11.0 kcal/mol. Since the barrier for O-O bond formation is 9.1 kcal/mol, this means

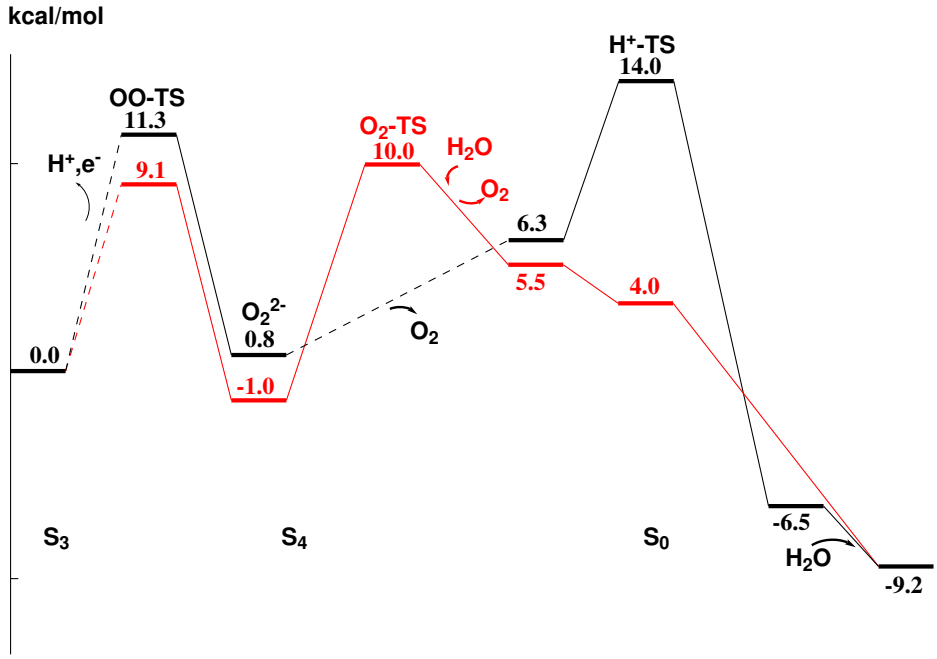

Figure 7: Energy diagrams for the transition from S_3 to S_0. The diagram for the previous mechanism is shown in black, the new one in red.

that the O_2 release step is still rate limiting with 11.0 kcal/mol. The rather high barrier for O_2 release means that this step remains a surprisingly demanding step of water oxidation, that has to be considered as potentially rate-limiting when designing artificial catalysts. Other steps in water oxidation like proton transfer and release, have probably not been fully optimized by nature in terms of individual rates, since they are not rate-limiting. It should otherwise have been relatively easy to increase the rate of these steps. A slow rate may even be advantageous to decrease back-flow of the electron to the reaction center.

b. Alternative O-O bond formation mechanisms.

Water exchange experiments have been among the most important experiments performed to date for elucidating the mechanism of water oxidation in PSII [30, 31, 32, 33, 34]. For example, these experiments were able to confirm the suggestion that the central oxygen **O5** in the OEC was one of the substrate oxygens forming O_2 [8]. This was the part that was most difficult to accept for the theoretically suggested O-O bond formation mechanism [6]. Prior to the more recent water exchange experiments, the early finding that both substrate oxygens exchange with water, with rates of 0.02 s^{-1} and faster, was instead used to discard the theoretical O-O bond formation mechanism, since model compounds did not show the same rate at all for exchange of oxo-groups [35, 36, 37]. However, the most recent

experiments showed that this exchange was indeed possible, which was also demonstrated by calculated exchange pathways [38].

If the situation can be considered solved for the slowly exchanging water substrate, the situation for the fast exchanging substrate still presents some mysteries. The theoretical mechanism indicates that in S_2 the fast exchanging substrate is present as a water derived molecule only very weakly bound to Mn1. Still, experiments show that the fast exchanging substrate at this stage exchanges with a rate as slow as 100 per second [31, 39]. This value appears to be incompatible with a water that is only weakly bound. Therefore, it has been suggested [40] on the basis of these experiments, that the fast exchanging substrate should rather be present as the hydroxide on Mn4, see Fig.5. A major problem with regard to the fast substrate as an hydroxide bound to Mn4 is that this requires the use of mechanisms C and D in Fig.8, where Mn4 will have an open site. It is difficult to conceive that an outside water, which should bind in this transition, could not bind directly to this open Mn4 site, at least to some extent, and thereby lead to a fast water exchange, faster than the one observed.

The solution to the above dilemma comes from recent mutation experiments [41]. It was shown that a mutation of Val185 by a phenylalanine led to a complete inability to evolve oxygen. Preliminary calculations, to be described elsewhere, indicate that the difference between a valine and a phenylalanine goes in the right direction but is not a major one in terms of energy. This means that the passage of water around Val185 is also quite difficult. Val185 must therefore be considered as a gate-keeper for water substrate binding to the OEC, a role valine has also in other enzymes such as nitrogenase [42]. An optimally functioning gatekeeper should just barely allow the desired substrate to get in and disallow all others. With this, the barrier for water binding should be only slightly faster than the rate-limiting step of oxygen evolution of a millisecond. This means that a slow exchange rate of 100 per second is indeed possible for a weakly bound water on Mn1, as suggested by previous calculations. However, it also means that a binding of a water to Mn4 could be prevented if the fast water substrate is an hydroxide bound to Mn4, as suggested experimentally. The two alternatives in S_2 will therefore only differ by the rate of the two processes. To determine which one is fastest requires very detailed calculations not yet done.

The above conclusions still leave two different mechanisms for O-O bond formation,

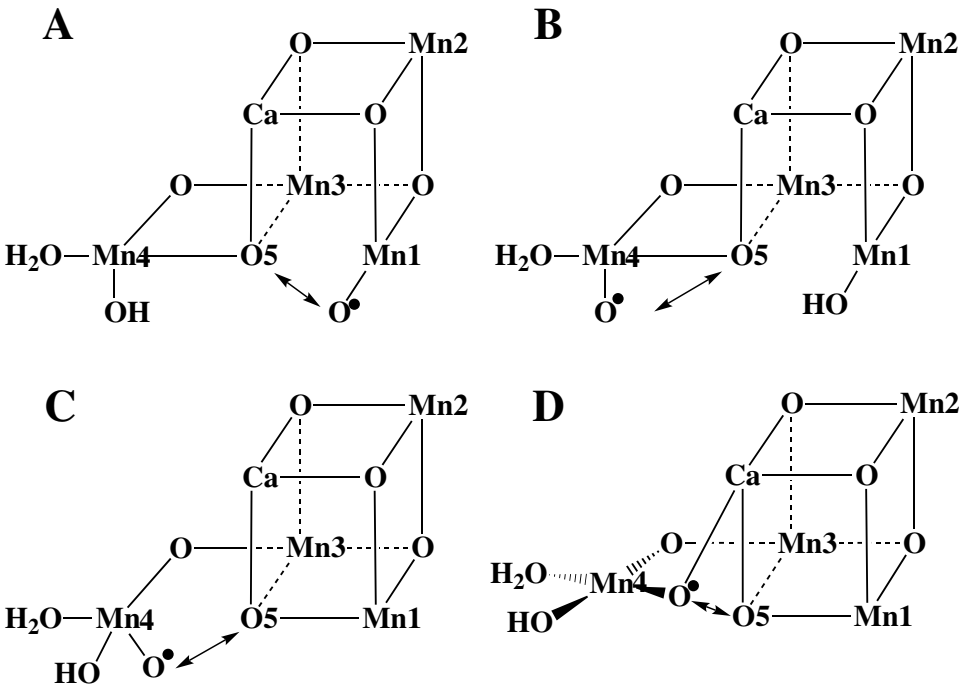

Figure 8: The four different transition states for O-O bond formation discussed here. A is the old "outer" oxo arrangement [10], and B is an alternative with "outer" oxo. C and D both have an "inner" oxo arrangement where C is the one suggested recently [43] modified compared to the original one based on experiments [44], and D is a present alternative with an "inner" oxo.

either occurring between an oxyl radical bound to Mn1 and O5, or between an oxyl radical bound to Mn4 and O5. These alternatives have been investigated here. In Fig.8, alternative A describes the previous mechanism suggested by theory [6, 7, 10]. This mechanism starts out from a structure of the S_3 state [1, 7, 10], which has now been confirmed by experiments [13]. In this structure, the O5 oxo forms bonds between Mn3 and the outside manganese Mn4, here termed the "outer" oxo arrangement. In the "inner" oxo arrangement, the O5 oxo instead forms bonds between Mn3 and Mn1. The "outer" oxo arrangement has been found to be superior in both S_2 and S_3 by theory [9, 7, 10] and by experiments [11, 13]. In fact, the experimental studies ruled out the "inner" structure for these states.

The first alternative mechanism tried here is the one labeled B in Fig.8. This mechanism starts out with the "outer" oxo arrangement, but now the fast water substrate is bound to Mn4 as suggested experimentally [43]. The hydroxide on Mn4 has in S_4 been oxidized to an oxyl radical in line with previous theoretical suggestions [6]. The transition state is shown in Fig.9. To be consistent with the original theoretical mechanism [6], the necessary

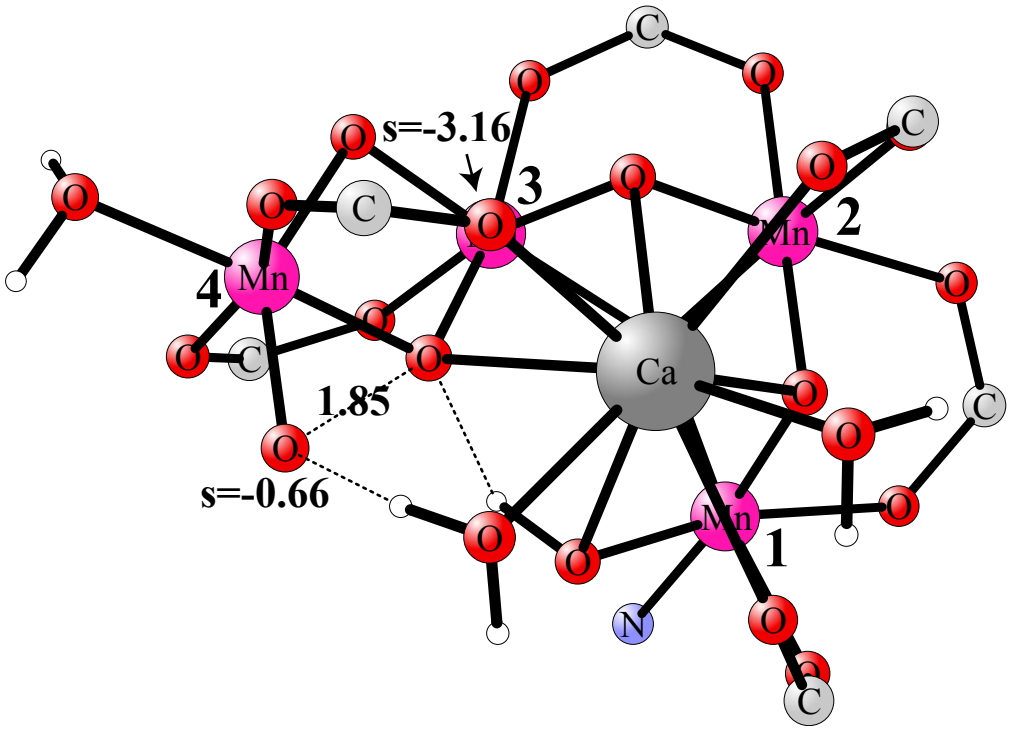

Figure 9: Transition state B (see Fig.8) for O-O bond formation with the "outer" oxo arrangement. Only the most important atoms are shown.

antiferromagnetic coupling is now made between Mn3 and Mn4, rather than between Mn4 and Mn1. The energy for this S_4 radical state is very high, 15.8 kcal/mol higher than for the one where the oxyl radical is bound to Mn1. At the TS, as shown in the figure, there is an O-O bond of 1.85 Å and the spins have started to change. The spin on the oxyl radical has gone down to -0.66 and the spin on Mn3 has decreased to -3.16. Since already the S_4 reactant is so high in energy, the barrier becomes as high as 31.8 kcal/mol counted from the optimal "outer" S_3 state, and this mechanism can therefore safely be ruled out.

The second alternative mechanism is the one directly suggested by experiments [43, 44]. In this mechanism, labeled C in Fig.8, the "inner" oxo arrangement is adopted. One reason for this could have been that this suggestion was made before the theoretical S_3 structure [10] was confirmed by experiments [13]. For this arrangement, no reasonable TS could be obtained.

In the final alternative mechanism, various attempts to find another TS with an "inner" oxo arrangement were made. It turned out that a much better TS was eventually found with a significantly lower energy than for the one originally suggested for the "inner" oxo arrangement. This mechanism is labeled D in Fig.8 and the TS is shown in Fig.10. A

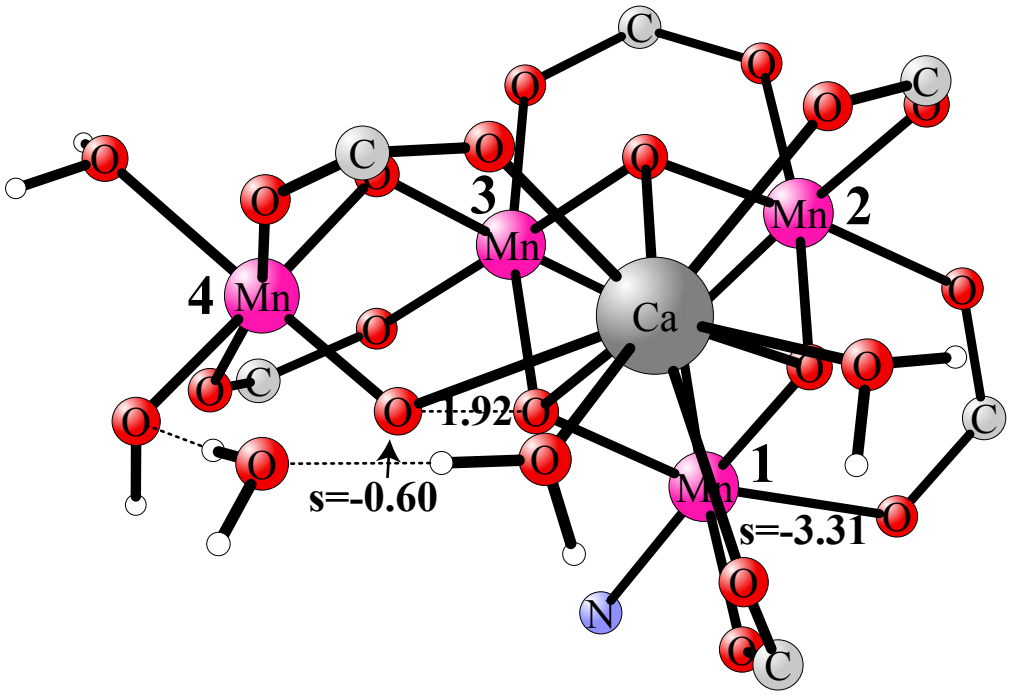

Figure 10: Transition state D (see Fig.8) for O-O bond formation with the "inner" oxo arrangement. Only the most important atoms are shown.

major structural change has occurred with a rotation of the ligand structure around Mn4 by about 30^o. The oxyl radical is now bridging between Mn4 and Ca which gives a substantial stabilization. Even though the S_4 reactant is still 5.2 kcal/mol higher than the reactant with the "outer" oxo arrangement with the radical bound to Mn4 by about 30^o, the energy of the TS is surprisingly low with only 10.2 kcal/mol, again counted from the optimal S_3 state. This makes it only 1.1 kcal/mol higher than for the one of mechanism A of 9.1 kcal/mol. In a previous comparison between these mechanisms, done before the high-resolution structure appeared, there was a much larger difference [7]. The two TS, for the "inner" and "outer" mechanisms, are extremely similar which is the reason for the similar barriers. Both mechanisms involve an oxyl radical and a bridging oxo, the same manganese atoms are involved with antiferromagnetic coupling between them, Mn1 and Mn4, and the O5 oxo group becomes part of the O_2 formed. The slightly more optimal angle between the bonds involved for the alternative "inner" TS almost compensates for the higher energy of the S_4 reactant.

It is clear that with such a small energy difference as 1.1 kcal/mol, model calculations cannot safely exclude the "inner" mechanism. For the "inner" mechanism to be viable, two rearrangements are necessary. First, the optimal "outer" S_3 arrangement has to be

transferred to an "inner" arrangement, involving moving the hydroxide bound to Mn1 to Mn4 in a process that simultaneously moves the O5 oxo from binding to Mn4 over to binding to Mn1. This step must be followed by a rotation of the ligand arrangement on Mn4 by 30^o. There are no indications at present that these two structural changes should be impossible. As discussed above, it is not possible to differ between these mechanisms based on the water exchange experiments for the fast substrate exchange either. More detailed experiments and more accurate model calculations would therefore be required.

In the recent combined spectroscopic/DFT study of the S_3 state [13], structures were suggested where an outside water forms hydrogen bonding bridges between the OH-group on Mn4 and a water molecule on calcium. This type of structures have been tested also here. The results using this arrangement were quite similar to the results obtained here, particularly for the relative energies. Concerning the absolute energies it is difficult to judge which arrangement is best, since a water molecule has to be taken from a position in the old structure and moved to the new position for obtaining comparable structures. The results will depend on which water molecule is moved and the results are not conclusive. The results will also depend on the arrangement of water in the third layer of the OEC, and this has not been fully optimized. With this background, the only conclusion that can be drawn is that the two different types of structures give very similar results.

IV. Conclusions.

A new mechanism has been found for the important O_2 release step in PSII. In the new pathway a transition state with a barrier height of 11.0 kcal/mol was located between the starting peroxide and a superoxide radical state. This TS was missed in the previous study, where this part of the O_2 release was assumed to be barrierless. Directly after the TS, an outside water moves into the central cavity of the OEC to replace O_2. This water enters much earlier than in the previous mechanism, which is an essential part of the new mechanism. In the next step, a change from a square pyramidal to trigonal bipyramidal structure occurs for the outer manganese Mn4, which is another important new feature. With this structural change it is now possible to move a proton from the central water to the hydroxide on Mn4 without any barrier. In contrast, this step was rate-limiting in the previous mechanism. Overall, the barrier for O_2 release has now gone down from the previous value of 14.0 to 11.0 kcal/mol.

Different alternative pathways for O-O bond formation have also been investigated in the present study. The previously suggested mechanism (A in Fig.8) remained the one with the lowest barrier. However, a mechanism starting out from the non-optimal "inner oxo" structure (D in Fig.8), with a rotation of the ligand coordination by about 30^o, was found to be only slightly less favorable. The mechanisms A and D are very similar with an oxo-oxyl bond formation involving the same manganese centra and with O5 as the oxo-part of the O-O bond.

Acknowledgements.

This work was generously supported by the Knut and Alice Wallenberg Foundation. X.L. thanks Beijing Normal University for support (2014NT10). Computer time was provided by the Swedish National Infrastructure for Computing.

References

[1] Siegbahn, P.E.M. *Chem. Eur. J.* **2008**, *27*, 8290-8302.

[2] Ferreira, K. N.; Iverson, T. M.; Maghlaoui, K.; Barber, J.; Iwata, S. *Science* **2004**, *303*, 1831-1838.

[3] Loll, B.; Kern, J.; Saenger, W.; Zouni, A.; Biesiadka, J. *Nature* **2005**, *438*, 1040-1044; Guskov, A.; Kern, J.; Gabdulkhakov, A.; Broser, M.; Zouni A.; Saenger, W. J. *Nat. Struct. Biol.* **2009**, *16*, 334-341.

[4] Umena, Y.; Kawakami, K.; Shen, J.-R.; Kamiya, N. *Nature* **2011**, *473*, 55-60.

[5] Suga, M.; Akita, F.; Hirata, K.; Ueno, G.; Murakami, H.; Nakajima, Y.; Shimizu, T.; Yamashita, K.; Yamamoto, M.; Ago, H.; Shen, J.-R. *Nature* **2015**, *517*, 99-103.

[6] Siegbahn, P.E.M. *Chem. Eur. J.* **2006**, *12*, 9217-9227.

[7] Siegbahn, P.E.M *Acc. Chem. Res.* **2009**, *42*, 1871-1880.

[8] Rapatskiy, L.; Cox, N.; Savitsky, A.; Ames, W.M.; Sander, J.; Nowacyzk, M.M; Rögner, M.; Boussac, A.; Neese, F.; Messinger, J.; Lubitz, W.; *J. Am. Chem. Soc.* **2012**, *134*, 16619-16634.

[9] Siegbahn, P.E.M. *Chem. Phys. Chem.* **2011**, *12*, 3274-3280.

[10] Siegbahn, P.E.M. *Biochim. Biophys. Acta* **2013**, *1827*, 1003-1019.

[11] Ames, W; Pantazis, D.A.; Krewald, V.; Cox, N.; Messinger, J.; Lubitz, W.; Neese, F. *J. Am. Chem. Soc.* **2011**, *133*, 19743-19757.

[12] Siegbahn, P.E.M. *Phys. Chem. Chem. Phys.* **2012**, *14*, 4849-4856.

[13] Cox, N.; Retegan, M.; Neese, F.; Pantazis, D.A.; Boussac, A.; Lubitz, W.; *Science* **2014**, *345*, 804-808.

[14] Siegbahn, P.E.M.; Crabtree, R.H. *J. Am. Chem. Soc.* **1999**, *121*, 117-127.

[15] Sproviero, E.M.; Newcomer, M.B.; Gascon, J.A.; Batista, E.R.; Brudvig, G.W.; Batista, V.S. *Photosynth. Res.* **2009** *102*, 455-470.

[16] Nilsson, H.; Rappaport, F.; Boussac, A.; Messingfer, J. *Nature comm.* **2014**, *5*, 4305.

[17] Gatt, P.; Stranger, R.; Pace, R.J. *J. Photochem. Photobiol. B: Biology* **2011**, *104*, 80-93.

[18] Krewald, V.; Retegan, M.; Cox, N.; Messinger, J.; Lubitz, W.; deBeer, S.; Neese, F; Pantazis, D.A. *Chemical Science* **2015**, *6*, 1676-1695.

[19] Blomberg, M.R.A.; Borowski, T.; Himo, F.; Liao, R.-Z.; Siegbahn, P.E.M. *Chem. Rev.* **2014**, *114*, 3601-3658.

[20] Becke, A. D. *J. Chem. Phys.* **1993**, *98*, 5648–5652.

[21] Reiher, M.; Salomon, O.; Hess, B.A. *Theor. Chem. Acc.* **2001**, *107*, 48-55.

[22] Siegbahn, P.E.M. *J. Biol. Inorg. Chem.* **2006**, *11*, 695-701.

[23] Siegbahn, P.E.M.; Himo, F. *J. Biol. Inorg. Chem.* **2009**, *14*, 643-651.

[24] Siegbahn, P.E.M.; Himo, F. in *Wire's Comput. Mol. Sci.* J. Wiley & Sons, Ltd. **2011**, Vol.1, 323-336.

[25] Grimme, S. *J. Chem. Phys.* **2006**, *124*, 034108; Schwabe, T; Grimme, S. *Phys. Chem. Chem. Phys.* **2007**, *9*, 3397-3406.

[26] Noodleman, L.; Case, D.A. *Adv. Inorg. Chem.* **1992**, *38*, 423-470.

[27] Siegbahn, P.E.M.; Blomberg, M.R.A. *Intern. J. Quantum Chem.* **2010**, *110*, 317-322.

[28] Jaguar 5.5, Schrödinger, L. L. C., Portland, OR, (1991–2003).

[29] Gaussian 09, Revision C.01, Frisch, M. J.; Trucks, G. W.; Schlegel, H. B.; Scuseria, G. E.; Robb, M. A.; Cheeseman, J. R.; Scalmani, G.; Barone, V.; Mennucci, B.; Petersson, G. A.; Nakatsuji, H.; Caricato, M.; Li, X.; Hratchian, H. P.; Izmaylov, A. F.; Bloino, J.; Zheng, G.; Sonnenberg, J. L.; Hada, M.; Ehara, M.; Toyota, K.; Fukuda, R.; Hasegawa, J.; Ishida, M.; Nakajima, T.; Honda, Y.; Kitao, O.; Nakai, H.; Vreven, T.; Montgomery, J. A., Jr.; Peralta, J. E.; Ogliaro, F.; Bearpark, M.; Heyd, J. J.; Brothers, E.; Kudin, K. N.; Staroverov, V. N.; Kobayashi, R.; Normand, J.; Raghavachari, K.; Rendell, A.; Burant, J. C.; Iyengar, S. S.; Tomasi, J.; Cossi, M.; Rega, N.; Millam, M. J.; Klene, M.; Knox, J. E.; Cross, J. B.; Bakken, V.; Adamo, C.; Jaramillo, J.; Gomperts, R.; Stratmann, R. E.; Yazyev, O.; Austin, A. J.; Cammi, R.; Pomelli, C.; Ochterski, J. W.; Martin, R. L.; Morokuma, K.; Zakrzewski, V. G.; Voth, G. A.; Salvador, P.; Dannenberg, J. J.; Dapprich, S.; Daniels, A. D.; Farkas, Ö.; Foresman, J. B.; Ortiz, J. V.; Cioslowski, J.; Fox, D. J. Gaussian, Inc., Wallingford CT, 2009.

[30] Messinger, J.; Badger, M.; Wydrzynski, T. *Proc. Natl. Acad. Sci.* **1995**, *92*, 3209-3213.

[31] Hillier, W.; Messinger, J.; Wydrzynski, T. *Biochemistry* **1998**, *37*, 306-317; Hillier, W.; Wydrzynski, T. *Biochim. Biophys. Acta* **2001**, *1503*, 197-209; Hillier, W.; Wydrzynski, T. *Phys. Chem. Chem. Phys.* **2004**, *6*, 4882-4889; Hillier, W.; Wydrzynski, T. *Coord. Chem. Rev.* **2008**, *252*, 306-317; Hendry, G.; Wydrzynski, T. *Biochemistry* **2003**, *42*, 6209-6217.

[32] Singh, S.; Debus, R.J.; Debus„ T.; Wydrzynski, T.; Hillier, W. *Philos. Trans. Roy Soc.* **2003**, *363*, 1229-1234.

[33] Hendry, G.; Wydrzynski, T. *Biochemistry* **2008**, *41*, 13328-13334.

[34] Noguchi, T. *Phil. Trans. R. Soc. B* **2008**, *363*, 1189-1195.

[35] Sproviero, E.M.; Shinopoulus, K.; Gascon, J.A.; McEvoy, J.P.; Brudvig, G.W.; Batista, V.S. *Phil. Trans. R. Soc. B* **2008**, *363*, 1149-1156.

[36] McConnell, I.L.; Grigoryants, V.M.; Scholes, C.P.; Myers, W.K.; Chen, P.-Y.; Whittaker, J.W.; Brudvig, G.W. *J. Am. Chem. Soc.* **2012**, *134*, 1504-1512.

[37] Dau, H.; Limberg, C.; Reier, T.; Risch, M.; Roggan, S.; Strasser, P. *ChemCatChem* **2010**, *2*, 724-761.

[38] Siegbahn, P.E.M. *J. Am. Chem. Soc.* **2013**, *135*, 9442-9449.

[39] Nilsson, H.; Krupnik, T.; Kargul, J.; Messinger, J. *Biochim. Biophys. Acta* **2014**, *1837*, 1257-1262.

[40] Lohmiller, T.; Krewald, V.; Navarro, M. P.; Retegan M.; Rapatskiy, L.; Nowacyzk, M.M; Boussac, A.; Neese, F.; Lubitz, W.; Pantazis, D.A.; Cox, N. *Phys. Chem. Chem. Phys.* **2014**, *16*, 11877-11892.

[41] Dilbeck, P.L.; Bao, H.; Neveu, C.L.; Burnap, L. *Biochemistry* **2013**, *52*, 6824-6833.

[42] Hoffman, B.M.; Lukoyanov, D.; Yang, Z.-Y.; Dean, D.R.; Seefeldt, L.C. *Chem. Rev.* **2014**, *114*, 4041-4062.

[43] Cox, N.; Messinger, J.; *Biochim. Biophys. Acta* **2013**, *1827*, 1020-1030.

[44] Messinger, J. *Phys. Chem. Chem. Phys.* **2004**, *6*, 4764-4771.